Journal of Molecular Catalysis A: Chemical 290 (2008) 1–14

Contents lists available at ScienceDirect

Journal of Molecular Catalysis A: Chemical

journal homepage: www.elsevier.com/locate/molcata

Editors' choice paper

An evaluation of the Noyori system "in reverse": Thermodynamic and kinetic parameters of secondary alcohol transfer dehydrogenation catalyzed by [(η^6-1-^{i}Pr-4-Me-C_6H_4)Ru(HN-CR′R″-CR′R″NTs)], R′ = H, Me; Ph, R″ = H, Me

Matthias Bierenstiel, Magdalena Dymarska, Ebbing de Jong, Marcel Schlaf*

Department of Chemistry, University of Guelph. The Guelph-Waterloo Center for Graduate Studies in Chemistry (GWC)^2, Guelph, Ontario N1G 2W1, Canada

ARTICLE INFO

Article history:
Received 28 November 2007
Received in revised form 3 May 2008
Accepted 17 May 2008
Available online 28 May 2008

Keywords:
Alcohol oxidation
Transfer hydrogenation
Ruthenium complexes
Catalysis

ABSTRACT

The 16 electron ruthenium complexes [(η^6-1-isopropyl-4-methyl-benzene)(X-N)Ru(II)], where X-N is 2-amido-1-ethoxide (**2**), 1-*N*-*p*-tosyl-1,2-diamido-ethane (**3**), 1-*N*-*p*-tosyl-1,2-diamido-benzene (**7**), 1-*N*-(*p*-tosyl)-1,2-diamido-1,1,2,2-tetramethyl-ethane (**8**) and 1-*N*-(*p*-tosyl)-1,2-diamido-*meso*-1,2-diphenyl-ethane (**9**) have been evaluated as catalysts for the transfer dehydrogenation of secondary alcohols to ketones in acetone and/or cyclohexanone solvent. Complexes **2** and **3** cannot be isolated and decompose under these conditions. In contrast complexes **7**, **8** and **9** are supported by ligands designed to resist β-hydride elimination and can with the exclusion of oxygen be held in solution for weeks. Complex **7** is not active as a catalyst. Complexes **8** and **9** are highly air-sensitive and active as catalysts for transfer (de)hydrogenations under oxidizing and reducing conditions, respectively. There is no coordinative inhibition of the catalysts by the ketone solvent under oxidizing conditions, but both catalysts show a correlation between the reaction rates and the ΔG values of the reactions with reactions leading to α, β-unsaturated ketones proceeding faster. For all alcohol/ketone substrate pairs where the ketone is not α, β-unsaturated, the hydrogenation reactions under reducing conditions (*iso*-propanol solvent) are at least one order of magnitude faster than the corresponding dehydrogenation reaction under oxidizing conditions (acetone solvent).

1. Introduction

1.1. Motivation

The reduction of ketones to secondary alcohols and the reverse, i.e., the oxidation of secondary alcohols to ketones are fundamental reactions in synthetic organic chemistry and an enormous variety of both stochiometric and catalytic methods have been developed [1,2]. In contrast there exist only few methods for the selective oxidation of *vic*-diols to the corresponding α-hydroxy-ketones [3,4]. In particular, viable methods for the oxidation of secondary hydroxyl functions in unprotected sugar polyalcohols [5] and furanose and pyranose sugars to give the corresponding furanuloses and pyranuloses are very rare [6,7]. A selective oxidation of *vic*-diols is challenging because the α-hydroxy-ketones are easily over-oxidized to diketones and ultimately carboxylic acids through oxidative C–C bond cleavage [4] and also tend to show uncontrollable secondary reactivity under the often either basic or acidic reaction conditions required by the oxidizing reagents employed.

One of the most active and versatile among the homogeneous catalytic *sec*-alcohol/ketone oxidation/reduction systems are the metal-ligand bifunctional ruthenium complexes of the type [(η^6-arene)Ru(XCH(C_6H_5)CH(C_6H_5)NH_n)Y] (arene = 1-^{i}Pr-4-Me-C_6H_4 or similar, X = O, NTs, Y = Cl, H or not present for n = 1, n = 1 or 2) developed by Noyori and co-workers [8–12]. While the application focus of these catalysts in their optically active forms has been on the highly successful enantioselective transfer hydrogenation of ketones using *iso*-propanol as both the solvent and reducing agent, Noyori and co-workers also demonstrated that the η^6-arene diamine ruthenium(II) based catalysts [(η^6-1-^{i}Pr-4-Me-C_6H_4)Ru(H)(1*R*,2*R*- NH(Ts)-CH(C_6H_5)CH(C_6H_5)NH_2)] (**1H**) or the corresponding hydrogen deficient 16 electron complex (**1**) can successfully be employed under oxidizing conditions (i.e., in acetone solvent) without the presence of a base. This allows the kinetic resolution of racemic benzylic or allylic alcohols achieving high ee values (92–99%) at 50% conversion of one alcohol enantiomer to the corresponding ketone within 6–36 h at 28 °C [13]. However to our knowledge only benzylic and allylic alcohols have been oxidized under the kinetic resolution conditions [13], while the transfer

* Corresponding author.
E-mail address: mschlaf@uoguelph.ca (M. Schlaf).

1381-1169/$ – see front matter © 2008 Elsevier B.V. All rights reserved.
doi:10.1016/j.molcata.2008.05.009

dehydrogenation of aliphatic alcohols or *vicinal* diols has not been reported in the literature.

2. Experimental

2.1. General

NMR spectra (400 MHz/^{1}H; 100 MHz/^{13}C) were measured in DMSO-d^6 with DMSO (δ 2.49, ^{1}H; δ 39.5, ^{13}C) and deuterated chloroform (δ 7.24, ^{1}H; δ 77.0, ^{13}C) as the internal reference unless indicated otherwise. NMR solvents were stored inside a dry-box under argon atmosphere over 4 Å activated molecular sieves. For variable temperature measurements the spectrometer temperature controller unit was calibrated using a bimetal thermometer directly inserted into the probe. DFT calculations were carried on a PC using the Gaussian 03 suite of programs. GC analyses were performed on a 30 m × 0.25 mm PEG column. The GC FID was calibrated for alcohol and ketone substrates with *cis*-decalin as an internal standard. GC–MS experiments were performed on a Varian 3800, Saturn 2000 a 30 m × 0.25 mm PEG column with 70 V electron impact ionization or acetonitrile chemical ionization technique. IR spectra were recorded with a Bomen FT-IR using a 1.0 and 2.0 mm CaF_2 liquid cell or a 15 μm cell containing a Teflon® washer (15 μm) between two BaF_2 cell windows. The IR cells were filled with the oxygen sensitive 16-electron complexes inside a glove box and carefully sealed from air atmosphere. Electron impact (EI) mass spectrometry was conducted on a JEOL HX110 double focussing mass spectrometer ionizing at 70 eV with source temperature at 200 °C. Electrospray ionization (ESI) mass spectrometry was conducted on a MicroMass QTOF Global Mass spectrometer in a positive ionization mode (3.5 kV spray voltage) at atmospheric pressure in acetonitrile. All experimental preparations were conducted in a dry-box under argon atmosphere and/or with usual Schlenk technique on a vacuum line. Acetone, *iso*-propanol and CH_2Cl_2 were dried by distillation under argon from anhydrous $CaCl_2$, anhydrous K_2CO_3 containing $LiAlH_4$ and K_2CO_3, respectively, degassed and stored under argon. Water was distilled under argon immediately before use. Alcohol and ketone substrates, *cis*-decalin and common solvents were purchased from commercial sources. All chemicals were reagent grade and used after degassing through repetitive freeze–thaw cycles. *N*-(*p*-tosyl)-1,2-diaminoethane [14], *N*-(*p*-tosyl)-*ortho*-diaminobenzene [15], 1,2-dinitro-1,1,2,2-tetramethylethane [16], 1,2-diamino-1,1,2,2-tetramethylethane [16], *meso*-1,2-diphenyl-1,2-diaminoethane [14] and *N*-(*p*-tosyl)-*meso*-1,2-diphenyl-1,2-diaminoethane [14,17] were prepared according to published literature procedures. *meso*-1,2-diphenyl-1,2-diaminoethane is commercially available.

2.2. Preparation of ligands and complexes

2.2.1. N-(p-Tosyl)-1,2-diamino-1,1,2,2-tetramethylethane (**5**)

In a 250 mL round bottle flask and with ice cooling, 1,2-diamino-1,1,2,2-tetramethylethane (9.5 g, 82 mmol) was dissolved in benzene (25 mL) and a solution of *p*-toluyl-sulfonyl chloride (5.2 g, 27 mmol) dissolved in 50 mL benzene was added drop-wise. After completion of the addition, the temperature of the reaction mixture was kept at 40 °C for 3 h, then increased to refluxing temperature for 30 min. After cooling to ambient temperature, white solids precipitated, which were filtered and dried *in vacuo* yielding 8.2 g of crude product. The product was dissolved in 1 M HCl (50 mL), filtered through celite and the remaining clear solution was cooled to 0 °C and 6 M NaOH (50 mL) was added carefully. The resulting white precipitate was filtered and dried *in vacuo*. 85% yield (6.2 g, 23 mmol). $C_{13}H_{22}N_2O_2S$, MM = 270 g mol^{-1}. ^{1}H NMR (DMSO-d^6; 2.49 ppm) δ 7.56 (d; J = 8.0 Hz; 2H), 7.11 (d; J = 8.0 Hz; 2H), 2.28 (s, br, 3H), 0.93 (s, 6H), 0.90 (s, 6H). ^{13}C NMR (DMSO-d^6; 39.5 ppm) δ 142.1, 138.0, 128.2, 126.1, 59.7, 55.7, 25.9, 23.6, 20.8. IR (KBr, cm^{-1}) ν 3383, 3246, 2979, 2427, 1910, 1598, 1579, 1457, 1387, 1362, 1299, 1218, 1180, 1151, 1107, 1048, 1015, 915, 810, 777, 687, 651, 557. High resolution MS (ESI, 3.5 kV spray voltage, m/z of M + 1): 271.1479. Monoisotopic molecular weight: 271.1480, average molecular weight: 271.394.

2.2.2. N-(p-Tosyl)-meso-1,2-diphenyl-1,2-diaminoethane (**6**) [14]

The compound was previously prepared by a different route in optically pure form (the NMR spectra match those published in reference [17]). *p*-Toluyl-sulfonyl chloride (0.64 g, 3.3 mmol) in 75 mL benzene was added drop-wise to a solution of *meso*-1,2-diphenyl-1,2-diaminoethane (2.12 g, 10 mmol) in 40 mL benzene and was stirred vigorously for 3 h. A white precipitate appeared and was filtered and treated with 1 M hydrochloric acid (∼50 mL). The remaining solid was filtered and filtrate made strongly basic by addition of NaOH pellets (∼4 g). A white crystalline solid appeared, was filtered, washed with 10 mL cold water and recrystallized from a benzene/hexanes mixture. Yield 48% (1.75 g, 4.8 mmol). $C_{21}H_{22}N_2O_2S$, MM = 366 g mol^{-1}. ^{1}H NMR ($CDCl_3$; 7.24 ppm) δ 7.38 (d, J = 7.8 Hz, 2H), 7.25–6.85 (m, 10H), 6.76 (d, J = 7.8 Hz, 2H), 5.60 (s, br, 1H), 4.39 (d, J = 5.6 Hz, 1H), 4.04 (d, J = 5.6 Hz, 1H), 2.24 (s, 3H), 1.57 (s, br, 2H). ^{13}C NMR ($CDCl_3$; 77.0 ppm) δ 142.9, 140.9, 137.1, 136.7, 129.2, 128.3, 128.2, 127.8, 127.7, 127.0, 126.9, 60.8, 63.4, 25.4. IR (KBr, cm^{-1}) ν 3057, 3020, 2962, 1599, 1493, 1447, 1382, 1261, 1080, 1071, 953, 811, 698, 666, 573, 545.

2.2.3. (η^6-1-Isopropyl-4-methyl-benzene)N-p-tosyl-ortho-diaminobenzene ruthenium(II) (**7**)

[*p*-Cymene $RuCl_2$]$_2$ (306 mg, 0.50 mmol) and *N*-(*p*-tosyl)-*ortho*-diaminobenzene (248 mg, 1.0 mmol) were transferred into a 30 cm long Schlenk tube with a stir bar. The Schlenk flask was evacuated and re-filled with Ar three times and 15 mL dry, under Ar distilled dichloromethane was added with a syringe. The red/orange solution was stirred for 10 min at room temperature and finely ground potassium hydroxide (0.5 g) was added. The reaction mixture was red coloured and stirred for additional 45 min at room temperature. Then, 15 mL of oxygen free water was added with a syringe and the white solid and excess KOH were dissolved. The greenish aqueous solution was removed with a canula and the remaining dichloromethane solution was dried with CaH_2 (∼0.4 g) until hydrogen gas evolution stopped. The solution was filtered from the remaining solids under Ar with a Schlenk frit. The solvent of the filtrate was evaporated under reduced pressure and a red solid was obtained in 82% yield (406 mg, 0.82 mmol). $C_{23}H_{25}N_2O_2SRu$, MM = 495.1 g mol^{-1}. Properties: The red complex is stable in air as a solid and in solution; soluble in dichloromethane, benzene, *iso*-propanol and acetone. ^{1}H NMR (CD_2Cl_2; 5.31 ppm) δ 9.49 (s, br, 1H), 7.74 (d, J = 8.0 Hz, 2H), 7.58 (d, J = 8.0 Hz, 2H), 7.21 (d, J = 8.0 Hz, 2H), 6.97 (dd, J = 7.6, 1.2 Hz, 1H), 6.74 (m, 2H), 5.67 (d, J = 6.4 Hz, 2H), 5.63 (d, J = 6.4 Hz, 2H), 2.57 (sept., J = 7.2 Hz, 1H), 2.35 (s, 3H), 2.22 (s, 3H), 1.24 (d, J = 6.8 Hz, 6H). ^{13}C NMR (CD_2Cl_2; 53.7 ppm) δ 151.5, 141.2, 139.5, 138.3, 128.1, 125.4, 119.0, 117.4, 116.3, 113.4, 100.6, 90.2, 79.6, 76.3, 30.9, 22.6, 20.1, 19.1. IR (KBr, cm^{-1}) ν 3299, 2962, 2360, 1476, 1456, 1321, 1307, 1140, 1086, 1036, 929, 847, 825, 665, 566.

High resolution MS (EI, 70 eV; m/z of parent ion, normalized) 490.0507 (13.25%), 491.0680 (4.23%), 492.0455 (6.00%), 493.0649 (31.23%), 494.0583 (39.14%), 495.0664 (50.87%). Monoisotopic molecular weight: 495.0680, average molecular weight: 494.580.

*2.2.4. (η^6-1-Isopropyl-4-methyl-benzene)-N-(p-tosyl)-1,2-diamino-1,1,2,2-tetramethyl-ethane ruthenium(II) (**8**)*

[*p*-Cymene $RuCl_2]_2$ (612 mg, 1.0 mmol) and *N*-(*p*-tosyl)-1,2-diamino-1,1,2,2-tetramethyl-ethane (540 mg, 2.0 mmol) were transferred into a 30 cm long Schlenk tube with a stir bar. The Schlenk flask was evacuate and re-filled with Ar three times and 30 mL of dichloromethane was added with a syringe. The red/orange solution was stirred for 10 min at room temperature and finely ground potassium hydroxide (1.0 g) was added. The reaction mixture immediately turned deep purple and was stirred for additional 15 min at room temperature. Then, 15 mL of oxygen free water was added via syringe and the white solid and excess KOH dissolved. The greenish aqueous solution was removed with a canula and the remaining dichloromethane solution was dried with CaH_2 (~0.8 g) until hydrogen gas evolution stopped. The purple solution was filtered under Ar with a Schlenk frit and the remaining solids were washed with 10 mL degassed dichloromethane. The solvent of the purple filtrate was evaporated under reduced pressure and a purple solid was obtained in 91% yield (914 mg, 1.82 mmol). $C_{23}H_{34}N_2O_2SRu$, MM = 503.7 g mol^{-1}. Properties: The purple solid is stable in air for a few hours, however, in solution the complex decomposes instantaneously upon exposure to air; soluble in dichloromethane, benzene, *iso*-propanol and acetone. ^{1}H NMR (C_6D_6; 7.15 ppm) δ 8.13 (d, J = 7.3 Hz, 2H, CH-tosyl), 6.94 (d, J = 7.3 Hz, 2H, CH-tosyl), 6.85 (s, br, 1H, N–H), 5.17 (d, J = 5.1 Hz, 2H), 5.05 (d, J = 5.1 Hz, 2H), 2.30 (sept., J = 6.8, 1H), 2.00 (s, 3H), 1.90 (s, 3H), 1.25 (s, 6H), 1.11 (d, J = 6.4 Hz, 6H), 0.73 (s, 6H). ^{13}C NMR (C_6D_6; 128.1 ppm) δ 147.6, 139.4, 128.7, 127.2, 98.7, 87.5, 82.5, 78.7, 74.1, 67.0, 32.0, 26.8, 24.6, 23.8, 21.1, 19.9. IR (KBr, cm^{-1}) ν 3281, 2960, 1598, 1492, 1470, 1387, 1352, 1254, 1127, 1087, 1052, 1025, 931, 807, 816, 791, 657, 561. High resolution MS (EI, 70 eV; m/z of parent ion; normalized) 498.1378 (1.19%), 501.1364 (2.92%), 502.1380 (3.70%), 503.1543 (5.35%), 504.1441 (8.33%), 505.1348 (2.79%), 506.1399 (5.01%), 507.1598 (1.46%). Monoisotopic molecular weight: 504.1384, average molecular weight: 503.652.

*2.2.5. (η^6-1-Isopropyl-4-methyl-benzene)-N-(p-tosyl)-1,2-diamino-meso-1,2-diphenyl-ethane ruthenium(II) (**9**)*

[*p*-Cymene $RuCl_2]_2$ (612 mg, 1.0 mmol) and *N*-(*p*-tosyl)-1,2-diamino-*meso*-1,2-diphenyl-ethane (728 mg, 2.0 mmol) were transferred into a 30 cm long Schlenk tube with a stir bar. The Schlenk flask was evacuated and re-filled with Ar three times and 30 mL of dichloromethane was added with a syringe. A bright red-orange precipitate formed after 5 min at room temperature and finely ground potassium hydroxide (1.0 g) was added. The red-orange precipitate dissolved and the reaction mixture was dark-red coloured. After additional stirring for 45 min at room temperature, 15 mL of oxygen free water (freshly prepared by refluxing under Ar atmosphere) was added via syringe and the white solid and excess KOH were dissolved. The brownish aqueous solution was removed via a canula and the remaining dichloromethane solution was dried with CaH_2 (~0.8 g) until hydrogen gas evolution stopped. The dark-red solution was filtered under Ar with a Schlenk frit and the remaining solids were washed with 10 mL degassed dichloromethane. The solvent of the dark-red filtrate was evaporated under reduced pressure and a red solid was obtained in 94% yield (1.12 g, 1.87 mmol). $C_{31}H_{34}N_2O_2SRu$, MM = 599.7 g mol^{-1}. Properties: The red solid is stable in air, however, a solution of the complex instantaneously decomposed upon exposure to air; soluble in dichloromethane, benzene, *iso*-propanol and acetone. Several recrystallization and isolation attempts of **9** failed with the material giving very complex ^{1}H NMR spectra. In the ^{13}C NMR spectrum broad overlapping signals observed, which coincide with characteristic chemical shifts of the other ruthenium complexes **7** and **8**. ^{1}H NMR (acetone-d^6, 2.09 ppm) 6.5–8.0 (br), 5.2–5.8 (br), 2.0–2.4 (br), 0.9–1.5 (br). ^{13}C NMR (acetone-d^6, 206.68 ppm, 29.92 ppm) 150–135, 124.7–122.1, 22.6, 20.1, 19.1. IR (KBr, cm^{-1}) ν 3057, 2961, 1917, 1598, 1494, 1447, 1382, 1261, 1081, 1071, 951, 811, 698, 664, 573, 545. High resolution MS (ESI, 3.5 kV spray voltage, m/z of M + 1, normalized) 595.1025 (5%), 598.0909 (28%), 599.0887 (40%), 600.0873 (50%), 601.0767 (100%), 602.0969 (15%), 603.0881 (40%), 604.1102 (5%). Monoisotopic molecular weight: 600.1384, average molecular weight: 599.732.

2.3. Kinetic experiments

The reactions were carried out in a 7 mL screw top vial equipped with a stir bar inside a glovebox under Ar atmosphere. GC-monitoring was conducted typically after 6 h, 24 h, 48 h, 72 h, 7 d and 14 d by direct injection of the crude reaction mixture.

2.3.1. Typical procedure under oxidizing/reducing condition

Alcohol/ketone substrate (1.0 mmol), 16-electron ruthenium catalyst (0.010 mmol) and *cis*-decalin (~50 mg) were dissolved in 5.0 mL acetone/*iso*-propanol in a 7 mL vial and stirred at room temperature. The reaction was monitored by quantitative GC using *cis*-decalin as the internal standard.

2.3.2. Typical procedure for equal-concentration experiments

Alcohol substrate (0.50 mmol), ketone substrate (0.50 mmol) and *cis*-decalin (~50 mg) were dissolved in 2.4 mL acetone (2.4 mL) and *iso*-propanol (2.5 mL). Then, 16-electron ruthenium complex (0.010 mmol) was added and the reaction mixture was stirred at RT. The reaction was monitored by quantitative GC using *cis*-decalin as the internal standard.

3. Results and discussion

3.1. Selection of catalyst system and oxidation substrates

The most active ruthenium catalysts for "forward" reactions, i.e., reductions of ketones in *iso*-propanol solvents, were obtained with β-amino-ethanol and *N*-tosyl-1,2-diaminoethane as the ligands [9]. Presumably the resulting complexes allow the most facile access of substrates to the catalytically active centre because of the least amount of steric repulsion with the ethylene backbone [9,11,18]. Cyclopentanol, cyclohexanol and 1,2;5,6-*O*-diisopropylidine α-D-gluco-furanoside (diacetone-glucose) were chosen as model systems for sugar substrates for an initial evaluation of β-amino-ethanol and *N*-tosyl-1,2-diaminoethane *p*-cymene ruthenium complexes as catalysts in hydrogen transfer reactions under oxidizing conditions, i.e., in acetone or cyclohexanone solvent.

3.2. Transfer dehydrogenation reactions with known systems

The results of the oxidation of cyclopentanol, cyclohexanol and diacetone-glucose with the β-aminoethanol *p*-cymene-ruthenium hydride complex (**2H**), which was synthesized according to literature procedure [18], are shown in Table 1. The oxidation reactions were monitored by quantitative GC using *N*-methyl-pyrrolidinone (NMP) as the internal standard. The experimental technique and actual activity of the catalyst was verified in a control experiment by the quantitative reduction of acetophenone to 1-phenyl-ethanol in *iso*-propanol after 6 h at room temperature using an authentic catalyst sample from the same synthesis batch [8].

In all oxidation reactions, the initial colour of the reaction solution is purple but turned to dark brown containing black

Table 1
Oxidation of secondary alcohols with *p*-cymene-Ru-β-aminoethanol hydride (**2H**) as the catalyst

Entry	Substrate	Solvent	Temperature (°C)	Time (h)	Conversion[a] (%)
1[b]	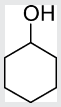	Acetone	25	48	<2
2[b]	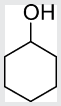	Acetone	56	24	15
3[b]	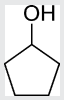	Acetone	25	48	<10
4[b]		Acetone	56	24	46
5		Cyclohexanone	25	48	40
6		Cyclohexanone	100	24	70
7	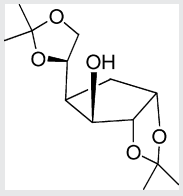	Acetone	56	24	0[c]
8	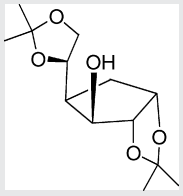	Cyclohexanone	100	24	12[d]
9	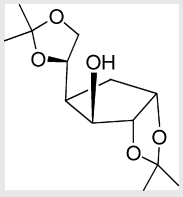	Cyclohexanone	150	24	71[d,e]

Reaction conditions: 1.0 mmol alcohol substrate, 0.1 mmol **2H** and NMP (~100 mg) in 10 mL ketone solvent under Ar.
[a] Production of ketone substrate determined by quantitative GC with NMP as internal standard.
[b] *In situ* generation of catalyst with additional 0.30 mmol KOH.
[c] Produced *iso*-propanol measured.
[d] Produced cyclohexanol measured.
[e] Isolation of sugar product failed.

precipitate after 24–48 h indicating the formation of ruthenium(0) as by-product of catalyst decomposition. Even at the very high catalyst load of 10 mol%, the room temperature oxidation of cyclohexanol and cyclopentanol in acetone solvent was very slow giving less than 15% conversion after 24–48 h (Table 1, entries 1,3,5). An increase in temperature to 56 °C (b.p. of acetone) increased the conversion of cyclopentanol and cyclohexanol to 15% and 46%, respectively. A higher temperature was reached when the ketone solvent was cyclohexanone, which is not only preferred as a higher boiling solvent but also releases ring strain energy upon formation of cyclohexanol [19]. With cyclohexanone as the hydrogen-acceptor, cyclopentanol was oxidized to cyclopentanone in 70% yield after 24 h at 100 °C (Table 1, entry 6). Diacetone-glucose was not oxidized with acetone as the hydrogen-acceptor at 56 °C but oxidation occurred with cyclohexanone at 100 and 150 °C with 12% and 71% of cyclohexanol produced, which as a first approximation should be equivalent to the amount of diacetone-glucose oxidized. However, isolation attempts of the product of

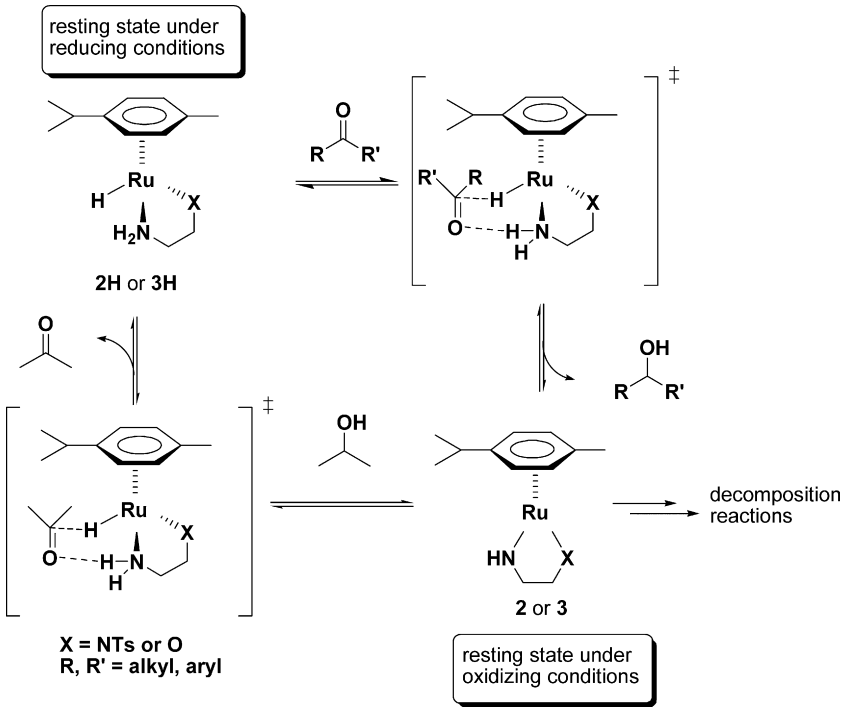

Scheme 1. Different resting states of catalysts **2** or **3** under reducing and oxidizing condition.

the diacetone-glucose reaction (Table 1, entry 9) failed and NMR analysis of the recovered solids revealed an intractable mixture of organic compounds generated through undefined side-reactions at the higher reaction temperature.

Important insights into the relative stability of the Noyori catalyst under reducing and oxidizing conditions in acetone or cyclohexanone solvent emerge from these results. Under reducing conditions in *iso*-propanol solvent the reaction mixture is yellow-orange coloured indicating that the resting state is the 18-electron ruthenium hydride complex **2H** as illustrated in Scheme 1. However, under oxidizing conditions in acetone or cyclohexanone solvent, the deep purple colour suggest that the 16-electron complex **2** is the dominant resting state (the same observations apply to the *N*-tosyl-1,2-diaminoethane complexes **3** and **3H**).

We next attempted to use the 16-electron complexes **2** and **3** directly as the catalyst in order to establish whether this would have a positive effect on the reaction rate as the initial step is the dehydrogenation of the alcohol substrate. The syntheses of the 16-electron β-aminoethanol and *N*-tosyl-1,2-diaminoethylene-*p*-cymene ruthenium complexes **2** and **3** (Chart 1) were conducted in analogy to the reported synthetic procedure [8]. However, the syntheses and isolation of both 16-electron complexes **2** and **3** failed. The purple colour of either 16-electron complex was briefly observed after addition of KOH to a CH_2Cl_2 solution of the chloro complexes **2Cl** and **3Cl** (cf. Scheme 1), but the reaction mixture turned black within minutes and undefined solids were obtained. We therefore hypothesize that the 16-electron complexes **2** and **3** undergo a β-hydride elimination reaction forming the imine and aldehyde based ligands as shown in Scheme 2, immediately followed by reductive elimination of the ligand leading to the complete disintegration of the complexes and formation of ruthenium(0). GC–MS analysis of the dark brown reaction mixture was however inconclusive as even with mild chemical ionization methods (acetonitrile) the presence of the very reactive imine and aldehyde intermediates could not be unambiguously determined.

Implicit in these observations is that during catalysis under reducing conditions, i.e., in *iso*-propanol solvent, the hydrogenation of the 16-electron complexes **2** and **3**, which by necessity must also be formed as reactive intermediates during the catalytic cycle, must be a lot faster than the ultimately destructive β-hydride elimination process.

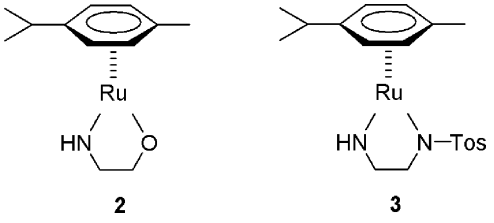

Chart 1. Structures of the 16 electron complexes β-amino-ethanol (**2**) and *N*-tosyl-1,2-diaminoethane (**3**) *p*-cymene-ruthenium(II).

3.3. Design and synthesis of oxidation resistant ligands

To avoid β-hydride elimination, the synthesis of oxidation resistant ethylene diamine ligands containing no β-hydrides or disfavouring a β-hydride elimination, was planned and executed. The three target ligands *N*-tosyl-*ortho*-diaminobenzene (**4**), *N*-tosyl-1,2-diamino-1,1,2,2-tetramethylethane (**5**) and *N*-tosyl-*meso*-diphenyl-1,2-diaminoethane (**6**) prepared as the racemic mixture, are shown in Chart 2.

While the diamino compounds **4** and **5** do not contain any β-hydrides, the *meso*-1,2-diphenyl ligand (**6**) contains two β-

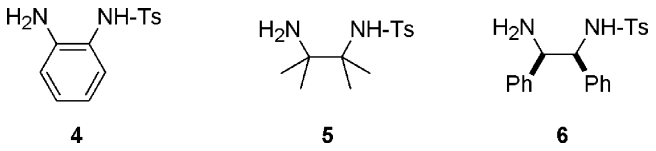

Chart 2. Degradation resistant ligands for the Noyori type catalysts.

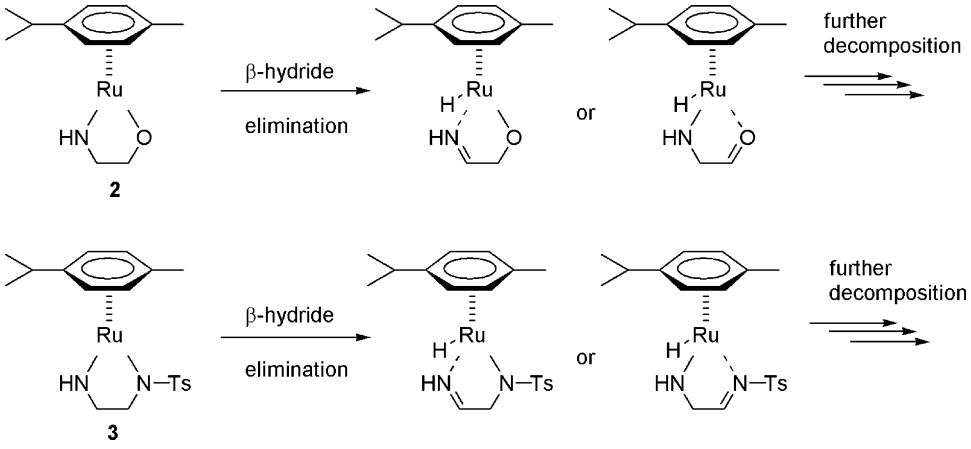

Scheme 2. Possible decomposition products of 16-electron complexes **2** and **3** through β-hydride elimination.

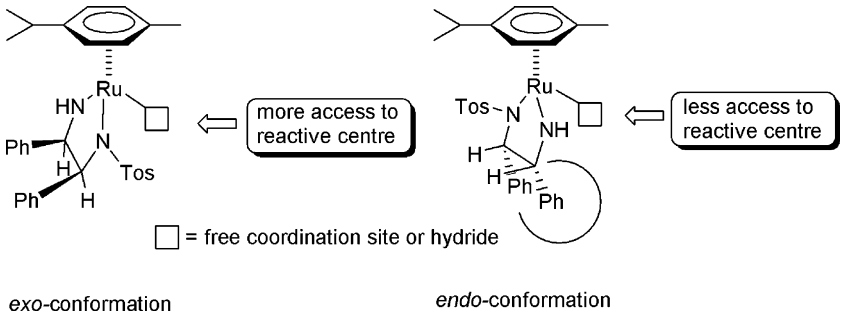

Fig. 1. *Exo*- and *endo*-conformation of *syn*-disubstituted 1,2-diaminoethane 16-electron ruthenium(II) complexes.

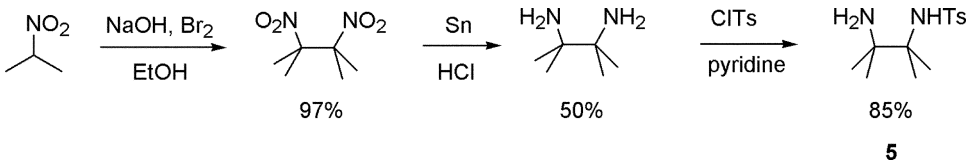

Scheme 3. Synthesis of *N*-tosyl-1,2-diamino-1,1,2,2-tetramethylethane (**5**).

hydrogen atoms. A β-hydride elimination from a 16-electron ruthenium complex of **6** was however not anticipated, as the complexes of the corresponding diastereomeric ligands (*R*,*R*- and *S*,*S*-configuration), which have an *anti*-arrangement of the phenyl substituents, have been shown to be stable under oxidizing conditions [13]. In the corresponding 18-electron complexes the *syn*-disubstituted 1,2-diaminoethane ligands should preferably coordinate to the ruthenium centre in an *exo*- rather than an *endo*-conformation as illustrated in Fig. 1. In the *exo*-position the phenyl ligands point away from the reactive catalytic centre thus enabling a more facile access of an ketone to the hydride ligand. By the same argument an alcohol would approach the ruthenium centre in a 16-electron complex in such a way that the *exo*-conformation of the hydride complex would be formed. The catalytic activities of the *syn*- and *anti*-disubstituted ligand are comparable [17], but the enantioselectivity of the reduction of aromatic ketones was generally decreased with optically pure *syn*-disubstituted ethylene ligands in η^6-arene ruthenium complexes compared to those in the *anti*-configuration. For the targeted non-enantioselective dehydrogenation reactions this is however not relevant and we postulated that the higher steric accessibility of the ruthenium centre imparted by the *syn-exo* arrangement of the phenyl ligands would result in a more active catalyst.

The synthesis of *N*-tosyl-*ortho*-diaminobenzene (**4**) was carried out by tosylation of *o*-amino-aniline following known literature procedures [15]. The new ligand *N*-tosyl-1,2-diamino-1,1,2,2-tetramethylethane (**5**) was prepared by a three step synthesis as shown in Scheme 3. The first step was the oxidative fusion of 2-nitro-propane to 1,2-dinitro-tetramethylethane in ethanol solvent with elemental bromine under basic conditions in 97% yield [16]. Subsequent reduction of the nitro groups to primary amines was effected by elemental tin in acidic medium. The resulting white solids were purified by steam distillation. Tosylation of the diamine compound with substoichiometric *p*-tosyl chloride in pyridine solvent gave **5** in 85% yield.

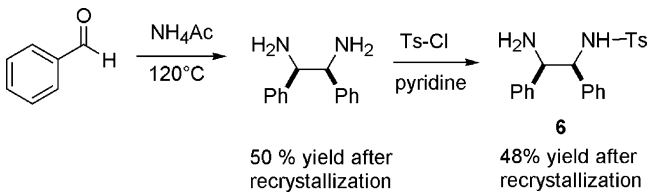

Scheme 4. Synthesis of *N*-tosyl-*meso*-1,2-diphenyl-1,2-diaminoethane (**6**).

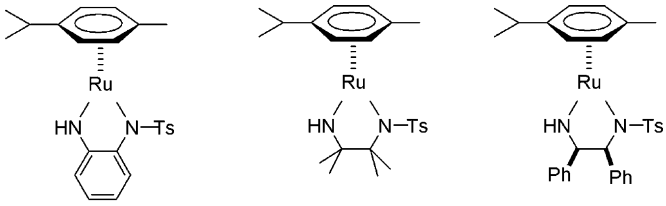

Chart 3. Structures of new β-hydride elimination resistant 16-electron ruthenium(II) complexes.

As outlined in Scheme 4 the precursor to the third ligand, *meso*-1,2-diphenyl-1,2-diaminoethane (**6**) was synthesized from the reaction of neat benzaldehyde and ammonium acetate under refluxing conditions in 50% yield after recrystallization from methanol [17,20]. The *meso*-1,2-diphenyl-1,2-diaminoethane compound obtained was subsequently mono-tosylated with substoichiometric amounts of *p*-toluyl-sulfonyl chloride in pyridine to give racemic *N*-tosyl-*meso*-1,2-diphenyl-1,2-diamino-ethane (**6**) in 48% yield.

3.4. Synthesis and properties of the new Noyori type complexes

The three *N*-tosyl-1,2-diamine ligands **4**, **5** and **6** were then used to prepare the corresponding 16 electron η^6-*p*-cymene ruthenium complexes **7**, **8** and **9**. Their structures are shown in Chart 3.

All three complexes were synthesized in analogy to published literature procedures [8,18]. The $[(p\text{-cymene})RuCl_2]_2$ precursor [21], synthesized from α-pinene and ruthenium(III) chloride hydrate in refluxing ethanol, was reacted with one equivalent *N*-tosyl-diamino ligand at room temperature in degassed dichloromethane under Ar atmosphere giving the chloro complexes, which can be isolated as solids in 82% (**7Cl**), 94% (**8Cl**) and 92% (**9Cl**) yield, respectively. The chloro complexes were however not characterized, but directly further reacted to the 16-electron complexes in the same solution. Addition of solid KOH, produced a bright red coloured reaction mixtures of the corresponding 16 electron complexes with **7Cl** and **9Cl** and a deep purple colour with **8Cl**. The compounds **7** and **8** are new compounds while **9/9H** have previously been generated *in situ* using the optically pure (1*S*,2*R*)-ligand enantiomer [17]. The tetramethyl complex (**8**) and *meso*-diphenyl complex (**9**) are both extremely air-sensitive when dissolved in organic solvents, but can with the rigorous exclusion of oxygen be held in solution for weeks while maintaining their catalytic activity. All three 16 electron complexes can be isolated as solids in very good to excellent yields and their identity and elemental composition is confirmed by high-resolution ESI mass spectra [22]. Complexes **7** and **8** give well defined ^1H and ^{13}C NMR spectra C_6D_6 and CD_2Cl_2, respectively, but the red solution of complex **9** in CD_2Cl_2 gives complex spectra showing a mixture of different species with four hydride peaks at −5.65, −5.87, −6.26 and −6.39 ppm (see Supplementary Material for images of NMR spectra of all three complexes). An integration of the hydride signals against all other protons present indicates that ∼22% of complex **9** is present in a hydride form, suggesting partial reaction to several different hydride complexes via a β-hydride elimination pathway (cf. Scheme 3). Complex **9** thus did not match our prediction of being resistant to β-hydride eliminations and behaves differently than the corresponding optically pure (1*S*,2*S*)-*N*-*p*-tolulenesulfonyl-1,2-diphenyl-1,2-diaminoethane based complexes with *anti* oriented phenyl substituents that result in well defined spectra and allowed a rare X-ray crystallographic structure determination of a 16-electron complex [8]. However, in contrast to complexes **2** and **3**, no brown or black precipitates formed over the course of several days. Instead solutions of complex **9** and its hydride derivatives maintain their red colour and NMR spectrum appearance for days, which prompted us to explore the catalytic activity of this material under both reducing and oxidizing conditions and compare it to that of complexes **7** and **9** (see below). During our study Wills and co-workers described the use of enantiomerically pure 1*S*,2*R*-**6** generating the corresponding 18-electron hydride complex in situ under reducing conditions, but gave no characterization data for this complex [17].

3.5. Hydrogen transfer reactions with degradation resistant ligands

The catalytic transfer hydrogenation activity of the *ortho*-diaminobenzene ruthenium complex **7** was investigated under both oxidizing and reducing conditions. A typical reaction was the oxidation of 1-phenyl-ethanol (1.0 mmol, 0.20 M) in 5.0 mL degassed acetone with 0.010 mmol (1 mol%) ruthenium complex **7** and *cis*-decalin as internal GC standard at ambient temperature and Ar atmosphere. No catalytic activity was observed with 1-phenyl-ethanol and cyclohexanol after 7 days. After 4 weeks, the contents of acetophenone and cyclohexanone were only ∼1%. For an investigation of the catalytic hydrogenation activity under reducing conditions, the same concentrations as under oxidizing conditions were employed with acetophenone (1.0 mmol, 0.20 M) as the substrate, 0.010 mmol (1 mol%) ruthenium complex **7** and *cis*-decalin in 5.0 mL degassed *iso*-propanol solvent at room temperature and under Ar atmosphere. Again the phenylene complex **7** showed no catalytic activity in reduction of acetophenone to 1-phenyl ethanol and only very marginal activity for the conversion of cyclohexanone to cyclohexanol (11% after four weeks). We attribute the low reactivity of **7** to the ability of the *ortho*-diaminobenzene to act as a *non-innocent ligand*, formally coordinating to the ruthenium centre as an *ortho*-quinone type system as illustrated in Scheme 5. This fundamentally alters the electronic environment of the ruthenium centre compared to the typical Noyori system and is reflected in differences of the NMR shifts of the arene ligand. The aromatic hydrogens of the cymene ligand have a chemical shift of 5.17 and 5.05 ppm in the tetramethyl-ruthenium compound **8** but in the *ortho*-diaminobenzene compound **7** the proton resonances are shifted downfield by approximately 0.5 to 5.67 ppm and 5.63 ppm, which indicates a higher ring current and thus more electron density donate towards the π*-orbitals of the cymene moiety. This electron density must originate from a more electron rich ruthenium centre than in the tetramethyl ruthenium complex, which in turn can be rationalized through the resonance structure **7′** on the right of Scheme 5, which postulates a ruthenium(0) centre.

Hydrogen transfer reaction under reducing and oxidizing conditions were carried out with a series of representative secondary alcohol/ketone pairs and the tetramethyl complex (**8**) as the catalyst. Standard conditions for the oxidation reactions were again alcohol (1.0 mmol, 0.20 M) in 5.0 mL degassed acetone with

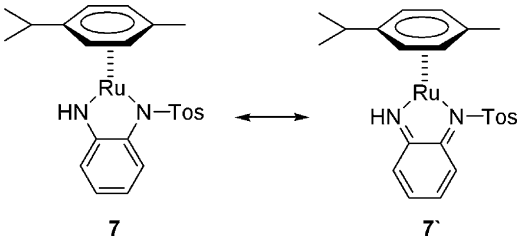

Scheme 5. *Ortho*-diaminobenzene acting as a non-innocent ligand on complex **7**.

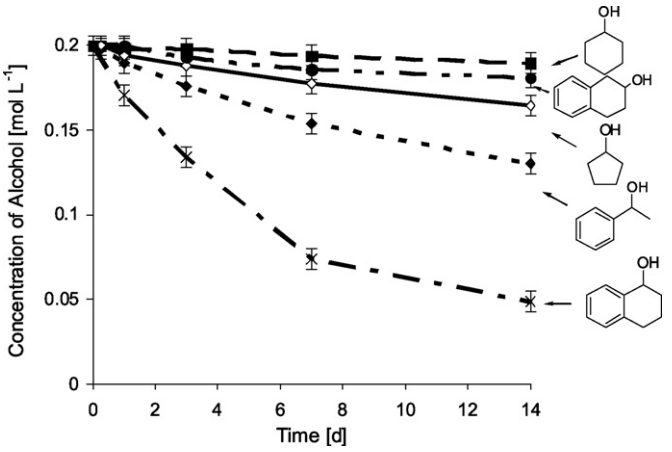

Fig. 2. Transfer dehydrogenation of secondary alcohols to ketones by **8**.

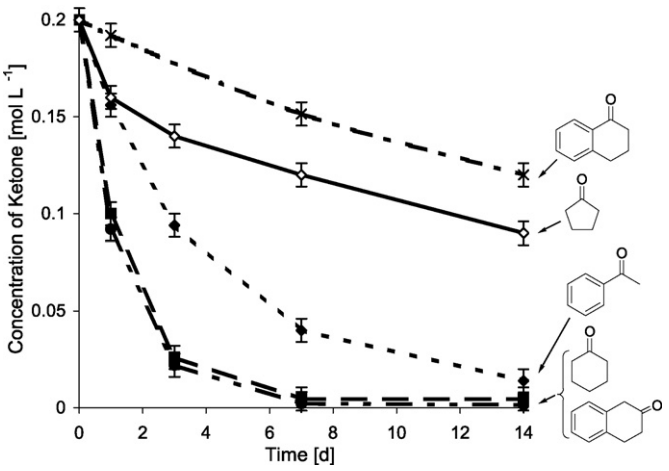

Fig. 3. Transfer hydrogenation of ketones to secondary alcohols by **8**.

0.010 mmol (1 mol%) ruthenium complex **8** at ambient temperature and Ar atmosphere and *cis*-decalin as the internal GC standard. The results of these oxidation reactions are shown in Fig. 2. The reducing conditions employed the same concentrations as the oxidizing conditions, but with ketone substrate in *iso*-propanol solvent. The results of the reductions are shown in Fig. 3. Under reducing conditions with *iso*-propanol as solvent and hydrogen source, the reaction mixture was yellow. In contrast, under oxidizing conditions the colour was deep purple.

The catalytic hydrogen transfer activity of **8** under reducing condition is much lower compared to the TON and TOF for **1**, **2**, or **3** reported by Noyori and co-workers, which reported a quantitative reduction of acetophenone to 1-phenyl-ethanol within 24 h [9,18]. The lower activity is likely a result of the steric hindrance by the four methyl groups present on the ethylene backbone in **8**. As shown in Fig. 3, cyclohexanone and β-tetralone were quantitatively reduced to their corresponding alcohols within ~5 d at room temperature and a 1 mol% catalyst load in *iso*-propanol solvent. After 14 d acetophenone reacted to 95%, cyclopentanone 52% and α-tetralone 37% to their corresponding alcohols. Under oxidizing conditions (Fig. 2) the order of reactivity is reversed compared to the reducing conditions and the catalytic activity is even lower and no quantitative oxidation of any substrate was observed even after 14 d. The 1-phenyl-ethanol content after 14 d is 69% compared to 82% of cyclopentanol. In order to probe the temperature response of catalyst **8**, reactions with the cyclohexanone/cyclohexanol and α-tetralone/α-tetralol substrate pairs were carried out under both reducing and oxidizing conditions at 22 and 50 °C. The data in Table 2 summarizes the results of these reactions. Under both oxidizing and reducing conditions the overall conversions of alcohol or ketone starting material of the hydrogen transfer reactions as well as the conversion after 24 h were increased at the elevated temperature. However, even at the higher temperature cyclohexanol was only 5% converted after 7 d compared to 3% after 7 d at room temperature.

Noyori and co-workers reported that the reduction of ketone substrates in *iso*-propanol solvent is first order with regards to the ketone. Similarly, the oxidation of allylic and benzylic alcohols in acetone solvent was first order in alcohol [13]. Thus assuming a

Table 2
Comparison of the performance of the ruthenium catalyst **8** under oxidizing and reducing conditions with complementary substrate/solvent pairs at 22 and 50 °C

Entry	Alcohol[a]	Temperature (°C)	Conversion[b] (%)	Entry	Ketone[c]	Temperature (°C)	Conversion[d] (%)
1	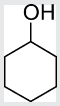	22	1% (24 h) 3% (7 d)	5	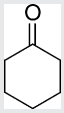	22	50% (24 h) 98% (7 d)
2	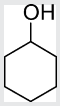	50	2% (24 h) 5% (7 d)	6	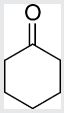	50	75% (24 h) 96% (48 h)
3	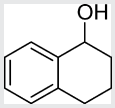	22	15% (24 h) 63% (7 d)	7	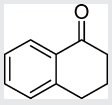	22	4% (24 h) 24% (7 d)
4	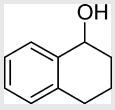	50	29% (24 h) 85% (7 d)	8	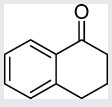	50	4% (24 h) 28% (7 d)

[a] *Reaction conditions*: 1.0 mmol alcohol, 0.010 mmol **8** and *cis*-decalin (~50 mg) in 5.0 mL acetone under Ar atmosphere.
[b] Determined by quantitative GC of produced corresponding ketone.
[c] *Reaction conditions*: 1.0 mmol ketone, 0.010 mmol **8** and *cis*-decalin (~50 mg) in 5.0 mL *iso*-propanol under Ar atmosphere.
[d] Determined by quantitative GC of produced corresponding alcohol.

Table 3
Rate constants for the catalytic alcohol/ketone transfer de/hydrogenation by **8** in acetone/*iso*-propanol solvent assuming a pseudo first order rate law

Entry	Alcohol/ketone	Temperature [°C]	Rate constant oxidation [s^{-1}][a,c]	Rate constant reduction [s^{-1}][b,c]
1	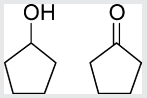	22	9.4×10^{-8}	6.4×10^{-7}
2	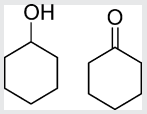	22	2.3×10^{-8}	6.3×10^{-6}
3	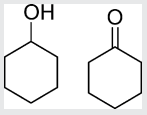	50	9.9×10^{-8}	1.9×10^{-5}
4	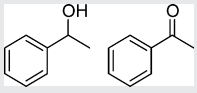	22	1.9×10^{-7}	1.4×10^{-6}
5	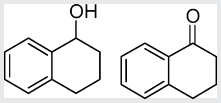	22	5.5×10^{-7}	2.3×10^{-7}
6	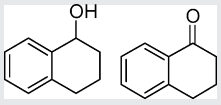	50	3.6×10^{-6}	5.7×10^{-7}
7	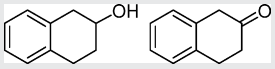	22	4.5×10^{-8}	1.7×10^{-6}

[a] *Reaction conditions:* 1.0 mmol alcohol, 0.010 mmol **8** and *cis*-decalin (~50 mg) in 5.0 mL acetone under Ar atmosphere.
[b] *Reaction conditions:* 1.0 mmol ketone, 0.010 mmol **8** and *cis*-decalin (~50 mg) in 5.0 mL *iso*-propanol under Ar atmosphere.
[c] Determined from quantitaive GC measurements and semi natural logarithmic plot of ln (concentration of product) vs. time [s].

pseudo first order rate law in alcohol under oxidizing condition and pseudo first order rate law in ketone under reducing condition we determined the corresponding rate constants from the concentration vs. time plots of the substrates as determined by quantitative GC (Figs. 2 and 3). Comparing the rate constants of the respective alcohol and ketone substrate pairs (Table 3) shows that the rates of the reductions are generally one to two orders of magnitude faster than the corresponding rates of oxidation. The exception is the α-tetralol/α-tetralone pair for which the oxidation reaction is markedly faster than the reduction, a fact that must be related to the formation of a benzylic conjugated carbonyl function upon oxidation of the alcohol. The implications of this phenomenon are discussed in greater detail in later sections (*vide infra*).

The tetramethyl complex **8** was also tested in the oxidation of *cis*-and *trans*-1,2-cyclohexanediol as the substrate (1.0 mmol) in 5.0 mL acetone and cyclohexanone solvent at room temperature under Ar atmosphere. However, after 7 d only trace amounts (<2%) of *iso*-propanol or cyclohexanol as well α-hydroxy-cyclohexanone substrate were detected. The reactivity of the diol substrate was in the same range as the oxidation of the cyclohexanol model system and thus further studies were focussed on the oxidation of the cyclohexanol model system.

Complex **9** was tested with the same cyclohexanol/cyclohexanone and α-tetralol/α-tetralone substrate pairs under oxidizing and reducing conditions using the same standard concentrations of 1.0 mmol substrate in 5.0 mL solvent, 1.0 mol% catalyst load and *cis*-decalin as the internal GC standard. Cyclohexanol was oxidized to cyclohexanone after 24 h only in trace amounts (<1%) and a 2% content was detected after 14 d at room temperature. In contrast, the same catalyst is much more active under reducing conditions 68% of cyclohexanone were reduced to cyclohexanol after 24 h, 88% after 48 and 95% after 72 h at room temperature. Under oxidizing conditions, α-tetralol was oxidized to α-tetralone in 20% after 24 h and 84% after 14 d at room temperature. In contrast, the reduction of α-tetralone yielded no reaction after 24 h and only 14% after 14 d. While the tetramethyl complex **8** is stable in solution for 3–4 weeks the diphenyl complex **9** starts to decompose after 2 weeks and a brown precipitate appears, presumably formed via the already discussed β-hydride elimination pathways.

3.6. Investigations into the coordinative inhibition of 16 electron complexes

We hypothesized that one possible reason for the slower oxidation reaction could be a coordinative inhibition of the catalysts (**8** and **9**) under oxidizing conditions through coordination of acetone or cyclohexanone solvent towards the Ru metal centre or amide/amine functionality of the catalyst (Chart 4). Coordination of acetone can in principle occur through an η^1 or η^2 coordination of the C=O function, both of which have been shown to occur at various metal centres [23,24], or by enolization of the acetone and cooperative coordination of the resulting C=C double bond and hydroxyl function.

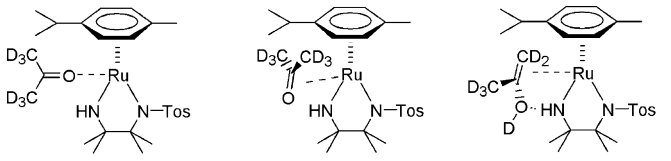

η^1-coordination of acetone to the Ru centre | η^2-coordination of acetone to the Ru centre | η^2-coordination of enol to the Ru centre

Chart 4. Conceivable inhibition of the catalyst through acetone-d^6 coordination.

This hypothesis was investigated by a series of NMR experiments. A sample of complex **8** was prepared in acetone-d^6 and scrambling of the amide proton (7.3 ppm) was observed at ambient temperature in less than 24 h. In benzene-d^6 and CD_2Cl_2 solvent no scrambling was observed. All three solutions remained purple in a sealed NMR tube for over 2 months at ambient temperature and no decomposition was observed. In $CDCl_3$ the complex decomposed to black precipitate after one week at room temperature. The scrambling of the amide proton can be explained through a rapid D/H exchange of acetone-d^6 with the amide through ketone-enol tautomerism of acetone in solution or through a possible η^2 coordination of the acetone enol to the Ru and NH moiety as shown in Chart 4. To further test this hypothesis, a low temperature ^2H NMR experiment with **8** was carried out in acetone-d^6 solvent at 400 MHz aiming to observe any olefinic signals of the complexed enol form of acetone. The sample was cooled to −80 °C and continuously shimmed observing the ^2H solvent signal. The sample was then allowed to thermally equilibrate at −80 °C for 15 min and the ^2H spectrum was recorded, however no olefinic ^2H signals were observed in the 3–6 ppm range. This means that the either there is no exchange of D/H with the amide function through the postulated η^2 coordination mechanism or it occurs so rapidly that even at −80 °C that the exchange of formed enol–Ru complex and surrounding acetone is still too fast to be observed on the time scale of the NMR experiment. To test for coordination of the non-enolized form of a ketone solvent, a ^{13}C NMR experiment was carried out with the same sample as well as cyclohexanone and complex **8**. For the second sample 30 mg of the 16-electron complex **8** was dissolved in 0.6 mL CD_2Cl_2, ten equivalents of cyclohexanone added and the ^{13}C NMR spectra recorded at room temperature. The ^{13}C NMR resonance of a carbonyl carbon complexed to a metal centre typically occur in the normal downfield range of carbonyl resonances for η^1 coordination but the resonances for η^2 coordinated carbonyl groups are observed in the upfield range of 45–110 ppm [23]. However, even with extensive data aquisition (4000 scans) no carbonyl resonances shifted from those of free cyclohexanone (211.5 ppm) could be observed in either experiment. In conclusion, all experimental NMR evidence suggested that the exchange of the NH-proton occurs very rapidly at room temperature and even −80 °C is too fast to be observed on the NMR time scale. In the ^{13}C and low temperature ^2H NMR experiment, no additional signals other than the free ketone were observed. NMR thus fails to provide any evidence for a coordinative inhibition of the 16-electron complex of **8** and **9** under oxidizing conditions.

In a corresponding IR experiment that in principle allows the investigation of carbonyl coordination to a metal centre on much faster time scales, the $\nu_{C=O}$ stretching frequency of acetone can be used as a sensitive probe for coordination of acetone in a η^1 or η^2 fashion, however η^1 coordination of a ketone to a metal centre lowers the $\nu_{C=O}$ usually less than 100 cm^{-1}. In contrast, with η^2 coordination of ketone to a metal centre the $\nu_{C=O}$ is observed in the range of 1017–1160 cm^{-1} due to the loss in bond order in carbon–oxygen bond [23,24]. One to ten equivalents of acetone were added to a dichloromethane solution containing complex **8** in a CaF_2 cell with 0.2 mm optical path length. No shift of the $\nu_{C=O}$ frequency was observed when comparing the IR spectrum of this sample to reference IR spectra of acetone or complex **8** recorded in dichloromethane. In another IR experiment complex **8** (10 mg) was dissolved in neat acetone (0.5 mL) and the IR spectrum was recorded using a cell with a very small (15 μm) optical path length. Even with this very short optical path length, the intensity of the $\nu_{C=O}$ stretching frequency was too strong so that the maximum bottomed out between 1707 and 1715 cm^{-1}. Again no shifted signal in the 1600–1700 cm^{-1} range or lower than 1600 cm^{-1} could be observed. On the basis of NMR and IR evidence we therefore conclude that the Ru centre of **8** is inert towards coordination by the acetone solvent and that the observed lower catalytic activity of the tetramethyl Ru complex in the oxidation reaction cannot be attributed to an inhibition of the 16-electron species by the surrounding ketone solvent.

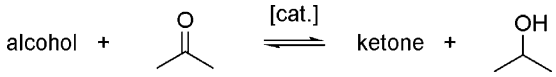

Scheme 6. Generic hydrogen-transfer reaction for calculation of ΔG°.

3.7. Thermodynamic investigations and models

In the absence of evidence for any coordinative inhibition of the catalysts under oxidizing conditions, our investigations centered on a thermodynamical approach in order to explain the slower oxidation vs. reduction rates. A full kinetic analysis aimed at gaining further insights into the reaction parameters was not attempted on the basis of the following considerations: As illustrated in Scheme 1, there exist two distinct resting states of the catalysts system in solution, the hydrogen deficient 16-electron complex **8** and the hydrogen loaded 18 electron complex **8H**. Effectively, there are therefore two different catalysts at different concentrations present in solution at any given time, the relative concentrations of which are a function of the redox potential and concentration of the participating alcohol/ketone pairs (both substrate and solvent). Determining these concentrations constitutes a major challenge to developing any kinetic model and to our knowledge no complete kinetic model and rate law taking this fact into account is available for the Noyori system. In consequence, we focused on thermodynamic parameters only, beginning with thermochemical calculations of the free reaction enthalpies of the isodesmic hydrogen transfer reactions. As the literature availability of experimental ΔG° values for the ketone/alcohol pairs selected by us is very limited, the relative free energies of the participating alcohol and ketone substrate with acetone and *iso*-propanol were determined through Gaussian 03 calculations by density functional theory [25]. The standard free energy of the transfer (de)hydrogenation of each alcohol with the acetone/*iso*-propanol pair, i.e., ΔG°, was calculated for the generic reaction shown in Scheme 6 and the equilibrium constants were calculated from $\Delta G^\circ = -RT \ln K$ at 298 K.

In order to correlate the calculated ΔG° results with the reaction actually carried out, $\Delta G_{reaction}$ was calculated for the conditions using Eq. (1) shown below. The initial concentration of alcohol substrate was 0.2 M and acetone solvent is present at 13.6 M. Plots of $\Delta G_{reaction}$ vs. the concentration of produced ketone are shown in Fig. 4.

$$\Delta G_{reaction} = \Delta G^\circ + \mathrm{RT}\ \ln Q,$$

$$Q = \frac{[\text{ketone}][\text{isopropanol}]}{[\text{alcohol}][\text{acetone}]},$$

$$[\text{ketone}]_{produced} = [\text{isopropanol}]_{produced} =: x = \frac{x^2}{[0.2 - x][13.6 - x]},$$

$$[\text{alcohol}]_{initial} = 0.2\,\text{M},\ [\text{acetone}]_{initial} = 13.6\,\text{M},\ T = 298\,\text{K} \qquad (1)$$

The calculated $\Delta G_{reaction}$ values for the majority of the alcohol and ketone substrate pairs pass through and cluster around the zero-line, i.e., they are essentially thermoneutral. However the values for the α-tetralol/α-tetralone, 1-phenyl-

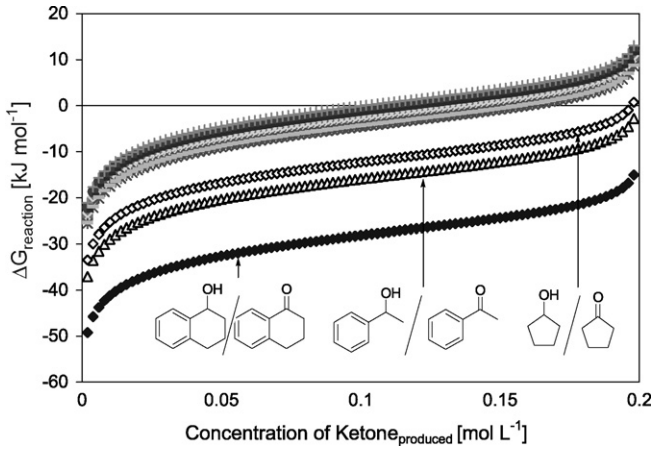

Fig. 4. $\Delta G_{reaction}$ calculated from DFT calculations as a function of produced ketone in acetone solvent from the corresponding alcohols. (♦) α-tetralone/tetralol, (◊) cyclopentanone/cyclopentanol, (Δ) acetophenone, 1-phenyl-ethanol.

ethanol/acetophenone and cyclopentanol/cyclopentanone pairs indicated in Fig. 4 are distinctively more negative suggesting that the equilibrium constitutes a quantitative oxidation of the alcohol to the corresponding ketone. These results are in principle congruent with the experimental values shown in Fig. 2, however the equilibrium for theses reactions had not been reached after 14 d. The results of the DFT calculations of $\Delta G_{reaction}$ for the reaction involving the reduction of ketones (0.2 M) in 5.0 mL *iso*-propanol (13.1 M) are displayed in Fig. 5 and also show a good correlation to the experimental data (Fig. 3). The reduction of α-tetralone is thermodynamically unfavoured and only a marginal α-tetralol content can be obtained at the equilibrium. The reductions of cyclopentanone and acetophenone are not as favoured as the other calculated ketone substrates, but the plots suggest that a quantitative conversion can be obtained at equilibrium.

Since the DFT calculations were carried out on the 6–31/g(d) level for the gas phase environment a finite error must be attributed to the calculated values. In solution hydrogen bonding does occur especially in *iso*-propanol solvent which further affects the minimum energies and will influence the $\Delta G_{reaction}$ values. However

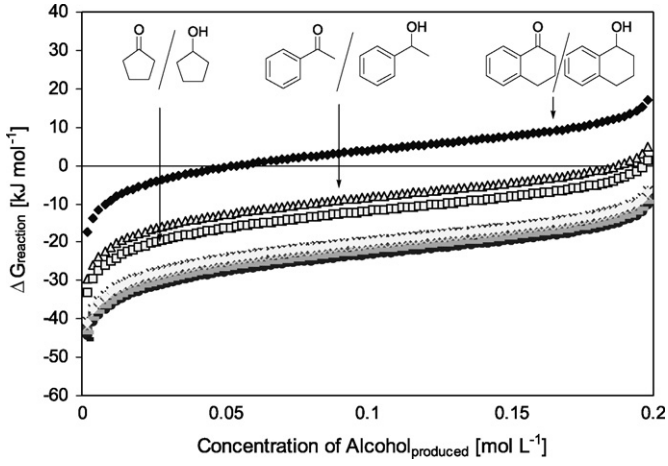

Fig. 5. $\Delta G_{reaction}$ calculated from DFT calculations as a function of produced alcohol in *iso*-propanol solvent from the corresponding ketone. (♦) α-tetralone/tetralol, (◊) cyclopentanone/cyclopentanol, (Δ) acetophenone, 1-phenyl-ethanol.

since the calculation of the $\Delta G_{reaction}$ values involves taking the differences of the absolute ΔG values for an isodesmic reaction, it is reasonable to assume that the errors cancel out at least partially minimizing their effect on the relative results (see below for a direct comparison of theoretical with experimental results).

From the experimental data (Tables 2 and 3) it is apparent that the reactions possessing a very negative ΔG° value in either oxidation or reduction direction were faster than those with lower ΔG° values. This observation suggests a relationship similar to the Hammond postulate, i.e., for the hydrogen transfer reaction under investigation, $\Delta G^\ddagger$ is correlated to ΔG°. With our observation that the resting state of the catalyst is dependent on the redox environment of the reaction partners involving solvents and alcohol and ketone substrates, the actual rate of reaction is then a superposition of the oxidation and reduction parameters for each of the two catalytically active species, i.e., one would expect substantially different rates for the forward and reverse reaction. As mentioned previously we refrained from trying to develop a full kinetic model for the Noyori system, as it would require a simultaneous knowledge of the actual relative concentrations of the two active catalysts species and the pairs ketones and alcohols present, which experimentally is difficult to realize [26]. In order to at least qualitatively detect the relative concentration of **8** in its 16-electron or 18-electron hydrogen loaded form, a simple experiment was carried out inside a glove-box under Ar atmosphere. Three solutions of **8** (5.0 mg) were prepared using (A) 5.0 mL acetone, (B) 5.0 mL *iso*-propanol and (C) a mixture of *iso*-propanol (2.5 mL) and acetone (2.5 mL). The acetone solution (A) was deep blue-purple coloured. The *iso*-propanol solution (B) was orange-yellow coloured after approximately 15 min at room temperature and the 1:1 acetone: *iso*-propanol mixture (C) was dark red-purple coloured. After addition of *iso*-propanol (1.0 mL) to (A) the colour changed slightly to a reddish-purple similar to the solution (C). A similar colour resulted in addition of acetone (1.0 mL) to (B). After addition of 15 mL of *iso*-propanol i.e. a 1:20 mixture acetone: *iso*-propanol, the colour intensity reduces due to concentration effect but there is no change back to a yellow colour. Addition of 15 mL acetone to (A) produced a deep purple solution with a taint of red. We therefore concluded that the 16-electron complex is the predominant species in any *iso*-propanol/acetone solvent mixture.

The kinetic data analysis was limited to determining the initial rates for the reaction, for which in a first approximation the reactant concentrations are known. Within this ultimately thermodynamic approach to the problem, there is however one single situation where there is no need in knowing the actual kinetic law of the reaction in order determine a correlation between ΔG° and initial rates. This situation arises, when both the oxidized and reduced substrate as well as the oxidizing and reducing solvent are present in equal concentrations [27]. At time t = 0 this is a condition easily realized experimentally. As expressed by Eq. (2), $\Delta G_{reaction}$ equals ΔG° at $t_{initial} = 0$, when the concentration of ketone and alcohol substrate as well the concentrations of acetone and *iso*-propanol solvent are set to be equal. Through cancellation of the respective concentration values Q is 1 and hence $\ln Q$ is zero. The combined ketone and alcohol concentration was set to 0.2 M with 0.010 mmol ruthenium catalyst in order to be able to compare results with the experimental and calculated data for the oxidation or reduction reactions. Another advantage of the equal concentration experiment is the direct experimental determination of ΔG° from the substrate and reactant concentration (by quantitative GC analysis) once the equilibrium has been established. The error margin for this determination is low as neither the numerator nor the denominator of the equilibrium constant equation, K is close to zero.

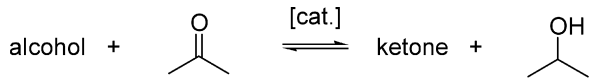

$$\Delta G_{reaction} = \Delta G^{o} + RT \ln Q$$

$$Q = \frac{[\text{ketone}]\,[\text{isopropanol}]}{[\text{alcohol}]\,[\text{acetone}]} = 1$$

$$[\text{ketone}]_{initial} = [\text{alcohol}]_{initial} = 0.1\ \text{M}$$
$$[\text{isopropanol}]_{initial} = [\text{acetone}]_{initial} = 7.4\ \text{M}$$

$$\Rightarrow \ln Q = 0$$

$$\Rightarrow \boxed{\Delta G_{reaction} = \Delta G^{o}} \qquad (2)$$

For the special situation of equal initial concentrations of all redox substrate pairs, it can also be assumed that the rate law for the forward reaction (Eq. (3)) and the rate law of the backward reaction (Eq. (4)) are only a function of the concentrations of ketone and alcohol and catalyst in its hydrogen loaded and unloaded form, respectively.

$$r_{forward}(t=0) = k_{forward} \times [\text{ketone}]_{initial} \times [\text{cat-H}_2] \qquad (3)$$

$$r_{reverse}(t=0) = k_{reverse} \times [\text{alcohol}]_{initial} \times [\text{cat}] \qquad (4)$$

In this situation, the free energy of the hydrogen transfer reaction of a given alcohol/ketone substrate pair can therefore be visualized experimentally. The overall direction of the hydrogen transfer reaction can easily be determined by quantitative GC measurements of the alcohol/ketone substrate concentration. The standard free energy, ΔG° can then be determined experimentally through calculation of the equilibrium constant K when the hydrogen transfer reaction has reached its equilibrium stage, i.e., the concentrations of the reactants do no longer change with time [28].

The initial rates also obtained from the equal concentration experiments are listed in Table 4 and are based on the observed production or consumption of alcohol substrate, i.e., under overall reducing condition ketone substrate reacts to the corresponding alcohol substrate. Thus the initial rate is >0. A "negative" initial rate in alcohol substrate indicates that the overall reaction favours the consumption of alcohol, i.e., oxidation of the alcohol substrate

Table 4
Initial rates and ΔG°_{exp} of equal concentration reactions with ruthenium catalysts **8** and **9**

Entry	Alcohol/ketone	Tetramethyl catalyst (**8**)		Entry	Diphenyl catalyst (**9**)	
		$\Delta G_{exp} \pm 5\%\ \Delta G_{exp}$ [kJ mol^{-1}][a]	Initial rate [10^{-9} mol L^{-1} s^{-1}][b]		$\Delta G_{exp} \pm 5\%\ \Delta G_{exp}$ [kJ mol^{-1}][c]	Initial rate [10^{-9} mol L^{-1} s^{-1}][d]
1		−0.03 ± 0.50	−1.3 ± 0.5	9	−0.35 ± 0.51	−4.6 ± 12
2	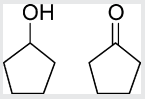	1.18 ± 0.52	76 ± 10	10	1.05 ± 0.52	229 ± 22
3	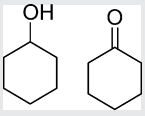	4.45 ± 0.87	127 ± 14	11	4.66 ± 0.91	235 ± 35
4	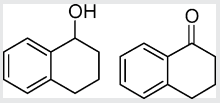	−10.32 ± 4.58	−223 ± 16	12	−3.33 ± 0.83	−257 ± 40
5	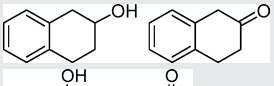	2.96 ± 0.65	158 ± 27	13	0.97 ± 0.52	103[d] ± 30
6	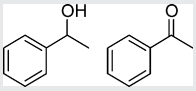	−1.69 ± 0.59	−24 ± 10	14	−0.20 ± 0.50	−2.6 ± 6.0
7	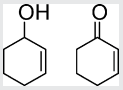	−11.46 ± 4.58	−281 ± 14	15	−1.78 ± 0.59[e]	−150 ± 10
8	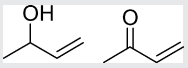	−11.46 ± 4.58	−332 ± 20	16	−5.72 ± 1.86	−476 ± 10

Reaction conditions: 0.50 mmol alcohol, 0.50 mmol ketone, 32 mmol acetone (2.3 mL), 32 mmol *iso*-propanol (2.4 mL), *cis*-decalin (~50 mg) and 0.010 mmol **8** or **9** at room temperature under Ar atmosphere.

[a] For error calculation see Supplementary Material.

[b] Error determined from first order exponential approximation.

[c] Approximated by first two data points.

[d] Catalyst decomposition after 7 d.

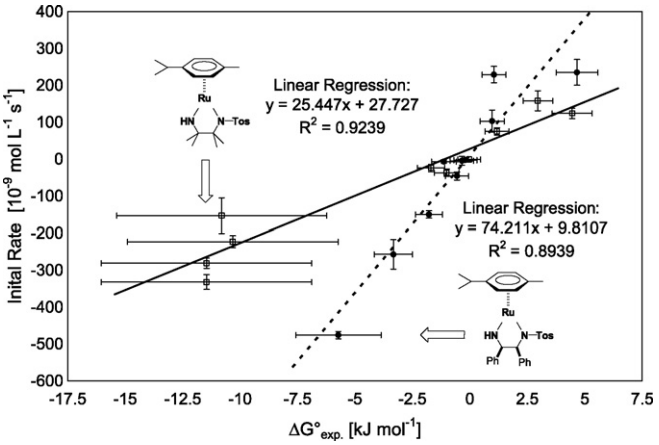

Fig. 6. Graph of initial rate vs. $\Delta G^{\circ}_{exp.}$ of equal concentration experiment with ruthenium catalysts **8** and **9**.

occurs. To evaluate the reliability of the initial rate constant, the standard deviation of the first order exponential fit of alcohol contents were used to calculate the error margins of the initial rates with a very conservative confidence interval. The initial rates also obtained from the equal concentration experiments were plotted against the experimental ΔG° value in order to visualize a potential relationship (Fig. 6). A linear regression was calculated for both ruthenium catalysts giving a correlation factor, R^2, of 0.92 and 0.89 respectively.

As the much faster oxidation of the secondary alcohols leading to the thermodynamically favoured α, β-unsaturated ketone shows, there clearly is a correlation between the thermodynamic driving force of the transfer dehydrogenation reactions and their relative rates. As the graphs in Fig. 6 suggest the correlation between the initial rates and ΔG° values is in fact linear, however no linear relationship between the logarithms of the rate constants and ΔG° values – as would be expected for a classic linear free enthalpy relationship – was found and at present we have no theoretical model to explain these results.

4. Conclusions

The oxidation of aliphatic and cyclic secondary alcohols in acetone solvent by Noyori type η^6-arene *N*-tosyl 1,2-diaminoethane based ruthenium(II) complexes with degradation resistant ligands proceeds only slowly and in low yield when compared to the reverse reduction reaction. The 16-electron amide complex is the resting state under oxidizing conditions and the 18-electron hydride complex under reducing conditions. A coordinative inhibition of the Ru or NH moiety of acetone solvent in an η^1-or η^2-fashion does not exist based on NMR and IR experiment evidence and is not the cause for the lower reactivity under oxidizing condition. The correlation of the initial rates of the alcohol consumption or alcohol production with the ΔG° of the participating alcohol/ketone pair gives an approximately linear relationship. The slope of this relationship is dependent on the catalyst employed. A possible explanation for the lower activity of the catalysts under oxidizing conditions compared to reducing condition is that there is a relatively high barrier of activation associated with the rearrangement of the 16-electron complex to a conformation required for hydrogen transfer and formation of the 18-electron hydride complex. Under oxidizing conditions, i.e., in excess ketone solvent, this formation of the 18-electron hydride complex becomes the rate determining step, while under reducing conditions, i.e., in excess alcohol solvent, the rate determining step occurs between the ketone substrate and the hydrogen loaded complex. Thus even though the overall reaction is a genuine equilibrium, the presence of two distinct active catalysts for the forward and reverse reactions gives rise to distinct reaction pathways with different activation barriers explaining the marked differences in reactivity in oxidation vs. reduction hydrogen transfer reactions. This difference in reactivity as well as an apparent inverse correlation between the initial rates of oxidation with the $\Delta G_{reaction}$ for hydrogen transfer reactions under oxidizing conditions, also renders the Noyori type system unsuitable for the catalytic synthesis of α-hydroxy-ketones from *vicinal* diols.

Supplementary data

Details and numeric results of thermochemical DFT calculations and equal concentration experiments. NMR data and spectrum images for all new ligands and complexes synthesized.

Acknowledgements

Funding for this research project was provided by University of Guelph, the Canadian Natural Science and Engineering Research Council (NSERC) and the Canadian Foundation for Innovation (CFI). M.B. would like to thank the Ernst Schering Research Foundation, Berlin, Germany for a doctoral stipend.

Appendix A. Supplementary data

Supplementary data associated with this article can be found, in the online version, at doi:10.1016/j.molcata.2008.05.009.

References

[1] M. Smith, March's Advanced Organic Chemistry: Reactions, Mechanism and Structure, sixth ed., John Wiley & Sons, New York, 2007.
[2] R.C. Larock, Comprehensive Organic Transformations: A Guide to Functional Group Preparations, second ed., Wiley-VCH, New York, 1999.
[3] S. Sakaguchi, D. Kikuchi, Y. Ishii, Bull. Chem. Soc. Jpn. 70 (1997) 2561–2566.
[4] M. Bierenstiel, P.J. D'Hondt, M. Schlaf, Tetrahedron 61 (2005) 4911–4917.
[5] I. Isaac, G. Aizel, I. Stasik, A. Wadouachi, D. Beaupere, Synlett (1998) 475–476.
[6] S. Freimund, A. Huwig, F. Giffhorn, S. Köpper, Chem. Eur. J. 4 (1998) 2442–2455.
[7] H.-M. Liu, Y. Sato, Y. Tsuda, Chem. Pharm. Bull. 41 (1993) 491–501.
[8] K.-J. Haack, S. Hashiguchi, A. Fujii, T. Ikariya, R. Noyori, Angew. Chem. Int. Ed. Engl. 36 (1997) 285–288.
[9] R. Noyori, S. Hashigushi, Acc. Chem. Res. 30 (1997) 97–102.
[10] M. Yamakawa, H. Ito, R. Noyori, J. Am. Chem. Soc. 122 (2000) 1466–1478.
[11] R. Noyori, M. Yamakawa, S. Hashiguchi, J. Org. Chem. 66 (2001) 7931–7944.
[12] R. Noyori, Angew. Chem. Int. Ed. 41 (2002) 2008–2022.
[13] S. Hashiguchi, A. Fujii, K.-J. Haack, K. Matsumura, T. Ikariya, R. Noyori, Angew. Chem. Int. Ed. Engl. 36 (1997) 288–290.
[14] M.T. Barros, F. Siñeriz, Tetrahedron 56 (2000) 4759–4764.
[15] H.-Y. Cheng, P.-H. Cheng, C.-F. Lee, S.-M. Peng, Inorg. Chim. Acta 181 (1991) 145–147.
[16] R. Sayre, J. Am. Chem. Soc. 77 (1955) 6689–6690.
[17] A. Hayes, G. Clarkson, M. Wills, Tetrahedron: Asymmetry 15 (2004) 2079–2084.
[18] J. Takehara, S. Hashiguchi, A. Fujii, S. Inoue, T. Ikariya, R. Noyori, J. Chem. Soc., Chem. Commun. (1996) 233–234.
[19] R.D. Bach, O. Dmitrenko, J. Am. Chem. Soc. 128 (2006) 4598–4611.
[20] N.A. Lozinskaya, S.E. Tkachenko, N.S. Zefirov, Russ. J. Org. Chem. 38 (2002) 1149–1153.
[21] M.A. Bennett, T.-N. Huang, T.W. Matheson, A.K. Smith, in: J.P. Fackler (Ed.), Inorganic Synthesis, John Wiley & Sons, New York, 1982, pp. 74–77.
[22] Repeated attempts to obtain conventional elemental analysis failed due to the air-sensitive nature of the complexes.
[23] Y.-H. Huang, J.A. Gladysz, J. Chem. Ed. 65 (1988) 298–303.
[24] F. Delbecq, P. Sautet, J. Am. Chem. Soc. 114 (1992) 2446–2455.

[25] Details of the calculation parameters as well as the numerical results are given in the Supplementary Material.
[26] NMR spectroscopy would be a logical choice here. However in our experience overlapping signals even at fields >400 MHz make the required accurate quantitation by integration effectively impossible.
[27] By using equal concentration for all reactants including solvents, the reaction is set-up in neutral. Thus depending on its ΔG° value the reaction itself determines if it "wants" to proceed into an oxidizing or reducing direction.
[28] Detailed descriptions of and data obtained from these experiments for all ketone/alcohol pairs are contained in the Supplementary Material.